

# Ionospheric and magnetic signatures of a high speed solar wind in low latitudes on 13 October 2012

Migoya-Orue, Y.O.<sup>1</sup>, Azzouzi, I.<sup>2,3</sup>, Coisson, P.<sup>4</sup>, Amory Mazaudier, C.<sup>2,3</sup>, Fleury, R.<sup>5</sup>, Radicella, S. M.<sup>1</sup>

- <sup>1</sup>. T/ICT4D, Abdus Salam International Centre for Theoretical Physics, Trieste, Italy
- <sup>2</sup>. LPP/UPMC/Polytechnique/CNRS, UMR 7648, University Pierre and Marie Curie Paris, France.
- <sup>3</sup>. LAZI /EMI/University Mohammed V Agdal Rabat, Rabat, Morocco.
- <sup>4</sup>. Institut de Physique du Globe de Paris, Sorbonne Paris Cité, Univ Paris Diderot, CNRS, Paris, France.
- <sup>5</sup>. MO-Dépt. Micro-Ondes//Lab-STICC/UMR CNRS 6285-Télécom Bretagne-Technopole de Brest-Iroise, Brest, France.

E mail (christine.amory@lpp.polytechnique.fr).

Accepted: 7 March 2016

**Abstract** This paper presents the impact of a fast solar wind on the ionosphere, in low latitudes, on 13 October 2012. On that day, the high speed solar wind reached the Earth around 16:00UT, during the recovery phase of a geomagnetic storm which started around 00:00UT. The solar wind speed was determined to be 580km/s, on the same day, around 17:00UT. Its impact was observed in low and equatorial latitudes, in Africa and in Eastern South America, on the F layer and on the geomagnetic field variations. Through the analysis of magnetic indices, ionosonde characteristics and the horizontal component of the geomagnetic field, we found that the 13 October 2012 event exhibited a local impact, affecting the observatories situated in a longitude sector between 315°E and 45°E. Particularly, the F layer in Africa (observed by the ionosonde at Ascension Island) did not present any lift, and there was a delay for approximately two hours of the ascent of the F layer in America (the ionosonde at Fortaleza). In this case, there was an evident inhibition on the development of spread F at the time of the Pre Reversal Enhancement (PRE) in Africa and Eastern America, while the ionograms of the days before and after presented clear spread F traces. The disturbances of the ionospheric equivalent electric current (Diono) deduced from the variations of the geomagnetic field at M'Bour near Dakar (Africa) and at Kourou (Eastern America) exhibited on the dayside, an anti Sq current which is signature of the influence of the Disturbance Dynamo Electric Field (DDEF).

© 2015 BBSCS RN SWS. All rights reserved

**Keywords:** equatorial ionosphere, geomagnetic storm, ionospheric disturbance dynamo, F layer, geomagnetic field, solar wind.

## 1. Introduction

Ionospheric variations constitute a key aspect within the complex field of space weather. The source of these changes of state in the ionosphere is in general related to variable solar wind conditions, solar disturbances, and meteorological influences. Trying to understand the effect of such variations is an important subject not only for practical applications but also for its intrinsic scientific relevance (Akala et al., 2012; Liu et al., 2011; Migoya-Orue et al., 2009). When ionospheric perturbations are associated with magnetic storms, they represent a real threat to the Global Navigation Satellite System (GNSS) signals (Lanzerotti, 2007). In middle latitudes, for example, the operation of space based augmentation systems (SBAS) can be endangered by the appearance of steep ionospheric gradients. The ionospheric effect on the GNSS is also significant in the regions surrounding the geomagnetic equator where the irregularities are more frequent and intense (Doherty et al., 2000). After sunset, a form of the Rayleigh-Taylor instabilities gives place to the Equatorial Plasma Bubble (EPB) formation (Kelley et al., 2009). The plasma irregularities produce in ionosonde

echoes a phenomenon called spread F, when the F layer is not presented at a single height but in a series of lines that are vertically 'swept'. The rise of the F layer due to the regular eastward electric field produces spread F/EPBs (Abdu et al., 1983).

Research to obtain predictions of the arrival of high speed solar wind streams (HSSWSs) by using observations from the Solar Terrestrial Relations Observatories (STEREOs) and the Advanced Composition Explorer (ACE) satellites are very promising (Davies et al., 2012), a fundamental understanding of the effects of HSSWSs emanated from coronal holes on the ionosphere, still remains a research effort (Grandin et al., 2015).

In the companion paper (Azzouzi et al., 2016), total electron content (TEC) data derived from the GNSS were employed in order to analyze the changes after the impact of a the HSSWS on 13 October 2012. In this work, we analyzed the same event but with the ionosonde and magnetometer data, being our purpose to complement the analysis done in the companion paper.

We present the source of the data sets and data processing (in section 2) and describe the results (in section 3). Section 3 is divided in three parts concerning the global context, the ionospheric and the geomagnetic signatures of the event. Section 4 is a discussion and then we present the conclusions (in section 5).

**2. Data set and data processing**

**2.1 Data set**

In this paper, we analyze the data of the month of October 2012 focusing on the period between 12 and 17 October. The data of the Solar and Heliospheric Observatory (SOHO) satellite ([www.nasa.gov/mission\\_pages/soho/](http://www.nasa.gov/mission_pages/soho/)) and the website: [www.spaceweather.com](http://www.spaceweather.com) were used to determine the solar sources of the disturbances (Coronal Mass Ejection (CME) and coronal hole). The observations of the ACE satellite (<http://omniweb.gsfc.nasa.gov/>) provide solar wind parameters: the solar wind speed and the north-south (Bz) component of the Interplanetary Magnetic Field (IMF). We analyzed various magnetic indices: AU, AL, AE, and Am/Km, the list of the Storm Sudden Comencement (SSC) from the International Service for Geomagnetic indices (<http://isgi.unistra.fr/>), and SYM-H index from the World Data Center for Geomagnetism, Kyoto (<http://wdc.kugi.kyoto-u.ac.jp>) (Mayaud, 1980; Menvielle et al., 2011).

Figure 1 provides the location of the magnetometers and the ionosondes. The geomagnetic data are obtained from the International Real-time Magnetic Observatory Network (INTERMAGNET) website (<http://www.intermagnet.org>) and the ionosonde data are from the Lowell GIRO Data Center (LGDC) website (<http://ulcar.uml.edu/DIDBase/>).

We used the ionosonde data of the Ascension Island observatory because only this observatory provides the regular data in the African region during our period of observations. Ascension Island is located in the Southern crest of the equatorial anomaly and large irregularities of plasma can be observed in its observations.

**2.2 Data processing**

Magnetic observatories located along the geomagnetic equator in the African sector (M'Bour (MBO) and Addis Ababa (AAE)), in the American sector (Huancayo (HUA) and Kourou (KOU)), and in the Asian sector (Guam (GUA)) are selected for this study and can be seen in Figure 1. We analyzed the variation of the horizontal geomagnetic component, H.

We took ten of the International Quiet Day (IQD) (<http://www.gfz-potsdam.de/en/section/earths-magnetic-field/services/kp-index/explanation/qd-days/>) in October 2012 to calculate the mean value of the averaged quiet  $\Delta H$  component of the geomagnetic field, computed as following:

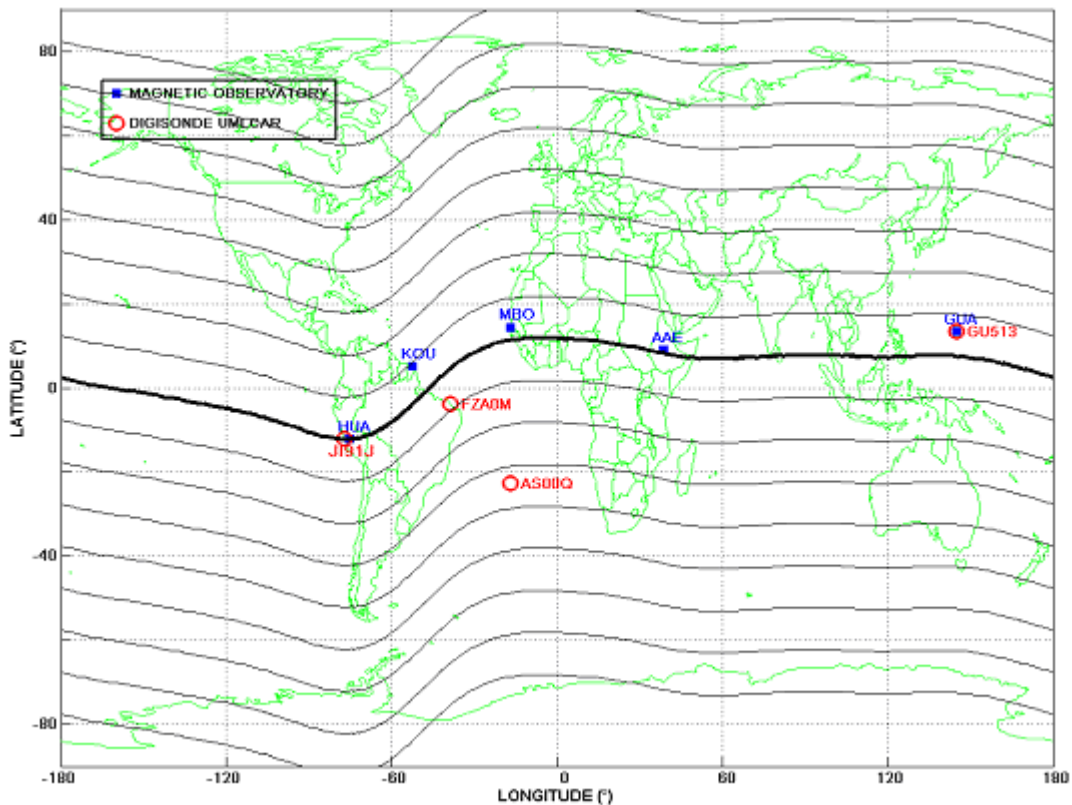


Figure 1. Location of the magnetometers and ionosondes

$$\Delta H_{quiet} = \frac{1}{n} \sum_{j=1}^n \Delta H_{quiet_j} \quad (1)$$

where  $n=10$ .

The baseline value ( $H_0$ ), which is the average of the hourly (LT) values around midnight was computed as follows:

$$H_0 = \frac{H_{22} + H_{23} + H_{24} + H_{01}}{4} \quad (2)$$

Thus, the daily range of  $\Delta H_i$  for every hour  $i$  was obtained by subtracting the baseline value,  $H_0$  from the hourly values  $H_i$ .

$$\Delta H_i = H_i - H_0 \quad (3)$$

where  $i=1$  to 24 hours.

The hourly  $Sq$  amplitude is subjected to non-cyclic variation, a phenomenon in which the value at 24LT differs from the one at 23LT (Vestine, 1967),

$$\Delta NC = \frac{H_{24} - H_{23}}{23} \quad (4)$$

Then, the solar quiet variation in  $H$ ,  $Sq(H)$  with adjusted values at the hours is given by:

$$Sq_i(H) = H_i + i\Delta NC \quad (5)$$

with  $i=1$  to 24 hours.

The magnetic disturbance due to ionospheric electric currents ( $D_{iono}$ ) is computed by the following expression given by Le Huy and Amory-Mazaudier (2005):

$$D_{iono} = \Delta H - SYMH \cdot \cos\lambda - Sq \quad (6)$$

where  $\Delta H$  is the  $H$  component variation recorded at one observatory,  $SYMH$  is the estimation of the ring current and  $\lambda$  is the geomagnetic latitude.

$D_{iono}$  is given also by the following relation:

$$D_{iono} = DP_2 + D_{dyn} \quad (7)$$

where  $DP_2$  is the magnetic disturbance related to the prompt penetration of magnetospheric electric field (Nishida, 1968; Vasyliunas, 1970) and  $D_{dyn}$  is magnetic disturbance related to the ionospheric disturbance dynamo (Blanc and Richmond, 1980; Le Huy and Amory-Mazaudier, 2005). In Fathy et al. (2014), a technique to separate the effect of the  $DP_2$  signal from the  $D_{dyn}$  signal has been proposed by taking running mean values from  $D_{iono}$ . For our case we took the moving average values every 3 hours.

### 3. Results

#### 3.1 Global context of the 13 October 2012 case

In October 2012, three major solar events affected the Earth. A CME hit the Earth at 05:26UT on 8 October 2012 and the impact was seen as a SSC. After this CME, two HSSWSs related to coronal holes arrived in the evening (~19:00UT) on 9 October and in the afternoon (~17:00UT) on 13 October. Figure 2 illustrates the

variation of various parameters of the solar wind and magnetic indices between 7 and 22 October (the solar wind speed in km/s, the  $B_z$  component of the IMF, the  $SYM-H$  indices and the  $AU$  and  $AL$  indices are shown from top to bottom panels). Two red arrows in the top panel show the arrival of the HSSWSs. The SSC is indicated by a red line in the  $SYM-H$  plot. On 13 October 2012, the second HSSWS arrived during the recovery phase of the storm around ~16:00UT. This storm started around midnight on 12 October with the southwards turning of the  $B_z$  component of the IMF. In this case, the HSSWS was associated to a decrease of  $SYM-H$  from ~-45 nT (~16:00UT) to ~-70 nT (~18:00UT) and an increase of the  $AL$  index (~1000 nT). The solar wind speed reached 570km/s around 17:00UT. On 18 October, there was a peak of the solar wind speed higher than 600km/s and there was not associated response of the magnetic indices,  $SYM-H$ ,  $AU$ , and  $AL$ . This can be explained by the fact that the  $B_z$  component of the IMF was small and not directed southwards during a long time like the other events on 8 and 13 October. There is detailed discussion on this figure in Azzouzi et al. (2016).

#### 3.2 Ionospheric signature ( $h'F$ and spread $F$ ) of the 13 October 2012 case

Figure 3 shows the variation of the virtual height of  $F$  layer,  $h'F$  at 4 MHz recorded by 4 ionosondes in the Asian sector (Guam), in the African sector (Ascension Island), and in the American sector (Fortaleza and Jicamarca). The  $h'F$  between 18LT and 24LT is plotted in this figure.

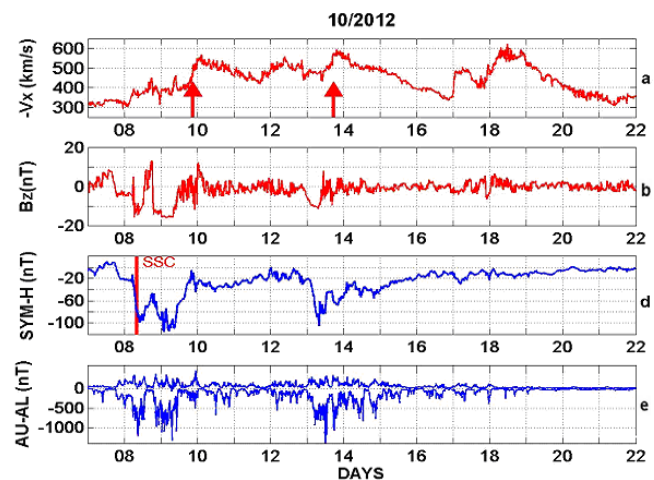


Figure 2. Variations of solar wind parameters ( $V_x$  and IMF  $B_z$ ) and magnetic indices ( $SYM-H$ ,  $AU$ , and  $AL$ ) between 7 and 22 October 2012. Two arrows in the solar wind speed show the arrivals of the HSSWSs. The red line on  $SYM-H$  plot indicates the time of the SSC.

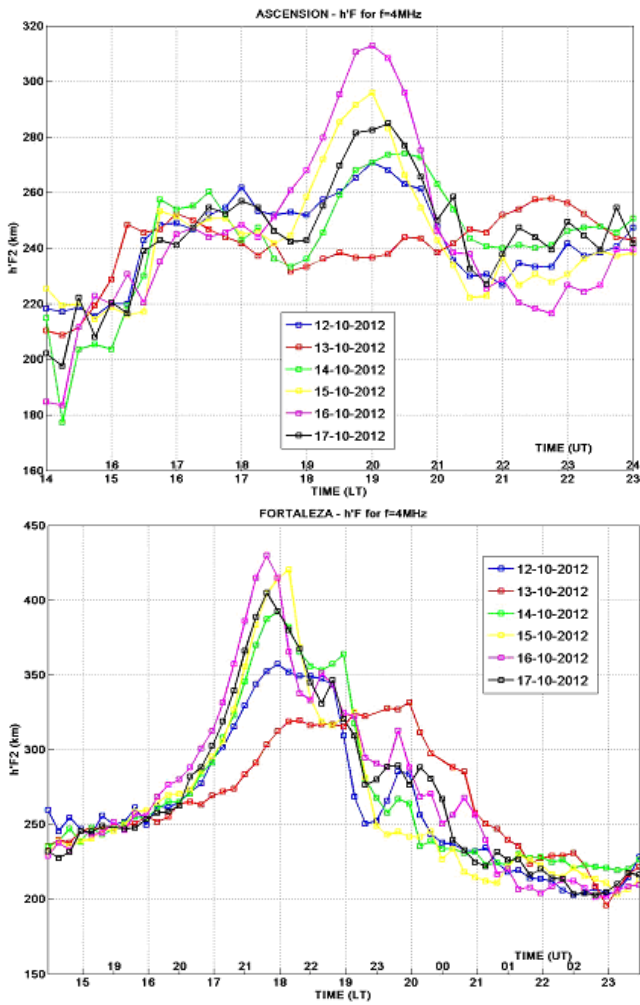


Figure 3a. Variation of the virtual height of the F layer at 4 MHz by the ionosonde observations every 15 minutes between 15LT and 24LT at Ascension Island and Fortaleza for the period between 12 and 17 October 2012.

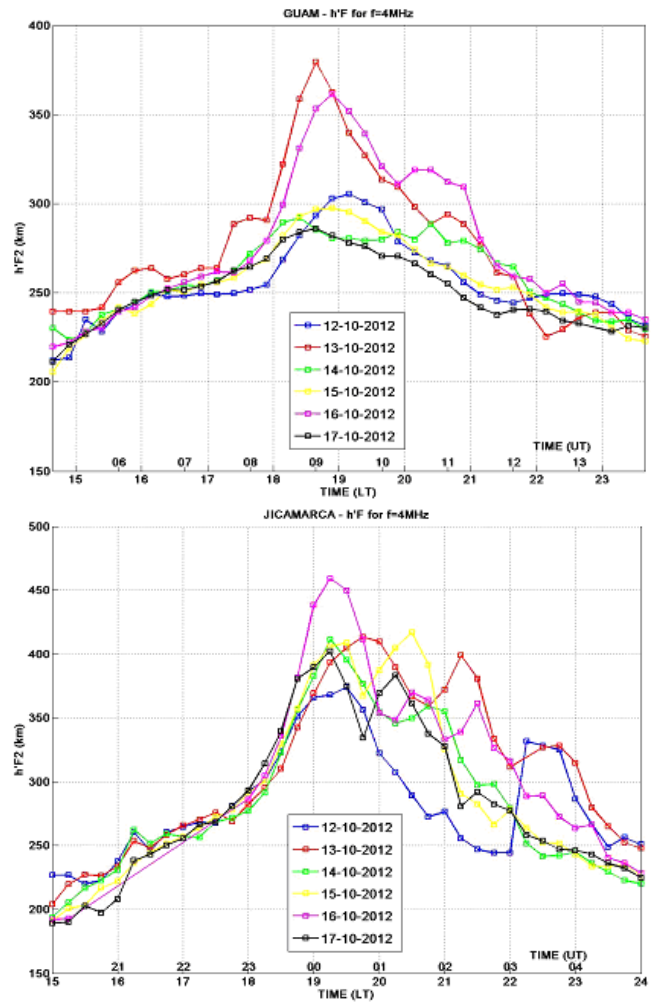


Figure 3b. Variation of the virtual height of the F layer at 4 MHz by the ionosonde observations every 15 minutes between 15LT and 24LT at Guam and Jicamarca for the period between 12 and 17 October 2012.

Table 1. Spread F observed at Ascension Island and at Fortaleza on 12, 13, and 14 October 2012

Day / Observatory	Ascension (LT = UT-1)	Fortaleza (LT = UT -3)
<b>12 October</b>		
Small spread F	20:30UT	20:50UT-21:10UT
High spread F	22:30-1:00UT	22:00-02:40UT
<b>13 October</b>		
Small spread F	23:45UT (1 ionogram)	No
High spread F	No	23:30-3:00 UT delay for approximately two- hours
<b>14 October</b>		
Small spread F	21:15-21:45 UT	21:30UT-22:00UT
High spread F	23:00-01:00UT	22:10-00:00UT & 00:40-02:10UT

Table 2. Maximums of H associated with geomagnetic storms

	GUA	AAE	HUA	MBO	KOU
<b>8 October</b>	- 170 nT	- 110 nT	- 90 nT	- 60 nT	- 40 nT
<b>9 October</b>	- 140 nT	- 100 nT	- 120 nT	- 120 nT	- 120 nT
<b>13 October</b>	- 120 nT	- 100 nT	- 60 nT	-7 0 nT(*)	- 80 nT
<b>14 October</b>	- 80 nT	- 50 nT	- 50 nT	- 80 nT	- 40 nT

(\*) last value registered before the gap

At Ascension Island (Figure 3a, top panel), there was no uplift of the F layer on 13 October. On the same day, at Fortaleza (Figure 3a, bottom panel), the F layer exhibited a behavior different from the other days of the period. The layer was lifted up later than the other days and the peak height of the F layer was lowest in the period. The F layer exhibited similar behavior at Ascension Island and Fortaleza on 13 October. This can be interpreted that both Ascension Island (LT=00T-1) and Fortaleza (LT=00T-3) were influenced by the HSSW. Ascension Island and Fortaleza are in different longitudes and their observations were slightly different. From Figure 3a, we think that Ascension Island was under the influence of the HSSWS between 17:00LT and 23:00LT and Fortaleza was affected between 16:30LT and 20:30LT. At Guam, on 13 October (Figure 3b, top panel), the h'F reached a maximum at 18:30LT. At Jicamarca, on 13 October (Figure 3b, bottom panel), the h'F exhibited a particular pattern with two maxima, the first maximum was around 19:45LT and another was around 21:15LT. The behavior on 13 October exhibited similar behavior as the majority of the other days of the period between 12 and 17 October. We notice that peaks of h'F of the four ionosondes were very high on 16 October (pink curve on each panel in Figures 3a and 3b) and the peak values were highest in the observations of Ascension Island, Fortaleza, and Jicamarca, respectively.

Figures 4 and 5 show the ionograms of Ascension Island and Fortaleza at 22:30LT (Figure 4) and at 19:30LT (Figure 5) on 12 (the top panels), 13 (the second panels), and 14 October (the bottom panels), respectively. According to Figures 4 and 5, it is clear that on 13 October, there was no spread F observed at Ascension Island and at Fortaleza. Table 1 gives the time of occurrence of the spread F at Ascension Island and at Fortaleza for the analyzed period. At Ascension Island, there was no spread F during the night except one ionogram at 23:45UT. At Fortaleza, the spread F appeared approximately two hours later on 13 October comparing with the appearances on 12 and 14 October. This delay corresponds to the delay of the ascent of the F layer (see Figure 3a, the bottom panel).

In the companion paper of this work, Azzouzi et al., (2016) found that the TEC rate of change index (ROTI), signature of the plasma irregularities, was negligible over the whole Africa on 13 October and was almost not observed over Eastern America. These observations are completely in agreement with the variation of the h'F observed at Ascension Island (Figure 3a, the top panel) and at Fortaleza (Figure 3a, the bottom panel).

The eastward equatorial electric field increases in the post sunset before it turns toward west during the night. This is called the Pre Reversal Enhancement (PRE) (Kelley, 2009). This eastward electric field combined to the horizontal magnetic field, produces an upward vertical drift  $V_z$  ( $E \times B$ ) which lifts up the F layer. This phenomena produces irregularities of the plasma observed by the ROTI on the GPS data and by spread F on the ionograms (Abdu et al., 1983). If there is no

ascent of the F layer, there is no production of irregularities nor spread F.

### 3.3 Geomagnetic signature of the 13 October 2012 case

Figure 6 shows the variations of the horizontal component of the geomagnetic field, H at GUA, AAE and HUA. On each panel, the blue line is the observation data and the red line is the regular variation computed following equation 3. On 8 October 2012, the impact of the CME was stronger at GUA (H~170 nT) than at AAE (H~110 nT) and at HUA (H~90 nT). H decreased as a function of local time. On 9 October, the impact of the first HSSWS was also larger at GUA (H~140 nT) than at AAE (H~100 nT) and at HUA (H~120 nT). For this event, the impact decreased with local time from GUA to AAE and then increased from AAE to HUA. On 13 October, the effect of the second HSSWS decreased as a function of local time like the impact of the CME. H was ~120 nT at GUA, was ~100 nT at AAE, and was ~50 nT at HUA. H of the 14 October disturbance was ~80 nT at GUA, was ~60 nT at AAE, and was ~50 nT at HUA. Figure 7 is similar to Figure 6 for the two magnetic observatories of MBO and KOU. These magnetic observatories are located in the crest of ionization of the northern hemisphere. MBO and KOU exhibited similar behavior. By the impact of the CME on 8 October, H was ~60 nT at MBO and was ~40 nT at KOU. By the impact of the first HSSWS on 9 October, H was ~120 nT at MBO and at KOU. During the impact of the second HSSWS on 13 October, the last H value recorded at MBO was ~70 nT. (Note that at MBO there is a gap in the data of about 8 hours from 14:00UT to 21:00UT, so we considered only the last value registered) and H was ~80 nT at KOU. On 14 October, H was ~80 nT at MBO and was ~40 nT at KOU. Table 2 summarized the results.

On 8 October, the impact of the CME was larger near the equator: GUA (H~170 nT), AAE (H~110 nT), and HUA (H~90 nT) than in the latitudes of the northern crest of ionization: MBO (H~60 nT) and KOU (H~40 nT). H at GUA was approximately three times greater than H at MBO and was approximately four times greater than H at KOU. This is explained by influence of magnetospheric currents which is stronger at the equator and decreases with increase of latitude. The SYM-H index largely varied from 8 October to the early morning on 9 October: -20 nT at 05:26UT, -100 nT at 10:00UT, -55 nT at 20:00UT, and -120 nT at 02:00UT. This is important to understand the large variation observed at the equatorial magnetic observatories.

When the first HSSWS impacted the Earth on 9 October, the SYM-H index was ~-20 nT and decreased to ~-40 nT. The amplitudes of the geomagnetic disturbance were almost the same order at GUA (H~140 nT), at AAE (H~100 nT), at HUA (H~20 nT), at MBO (H~120 nT), and at KOU (H~120 nT). This can be explained by the fact that the ionospheric electric currents are stronger than the magnetospheric electric currents.



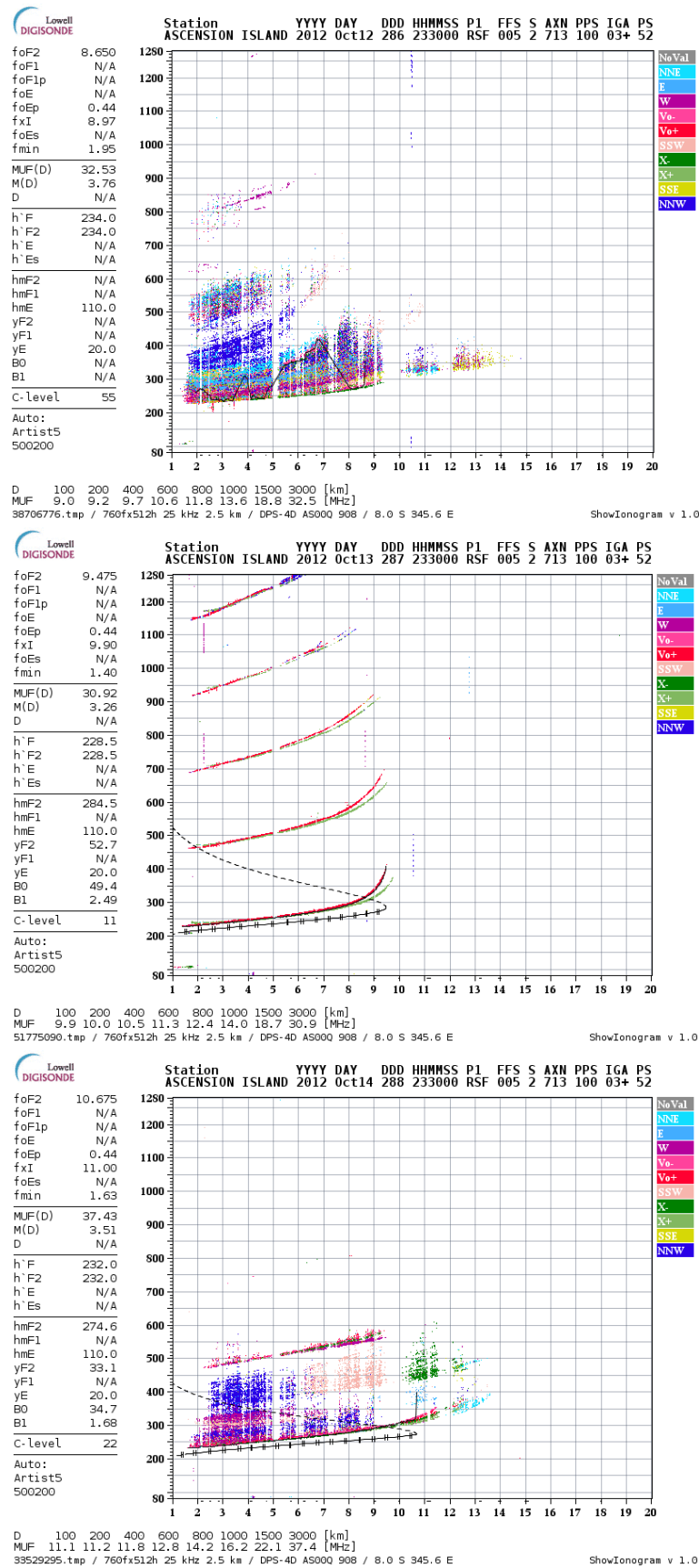


Figure 4. Ionograms of Ascension Island at 22:30LT (23:30UT) on 12 (the top panel), 13 (the middle panel), and 14 (the bottom panel) October 2012.

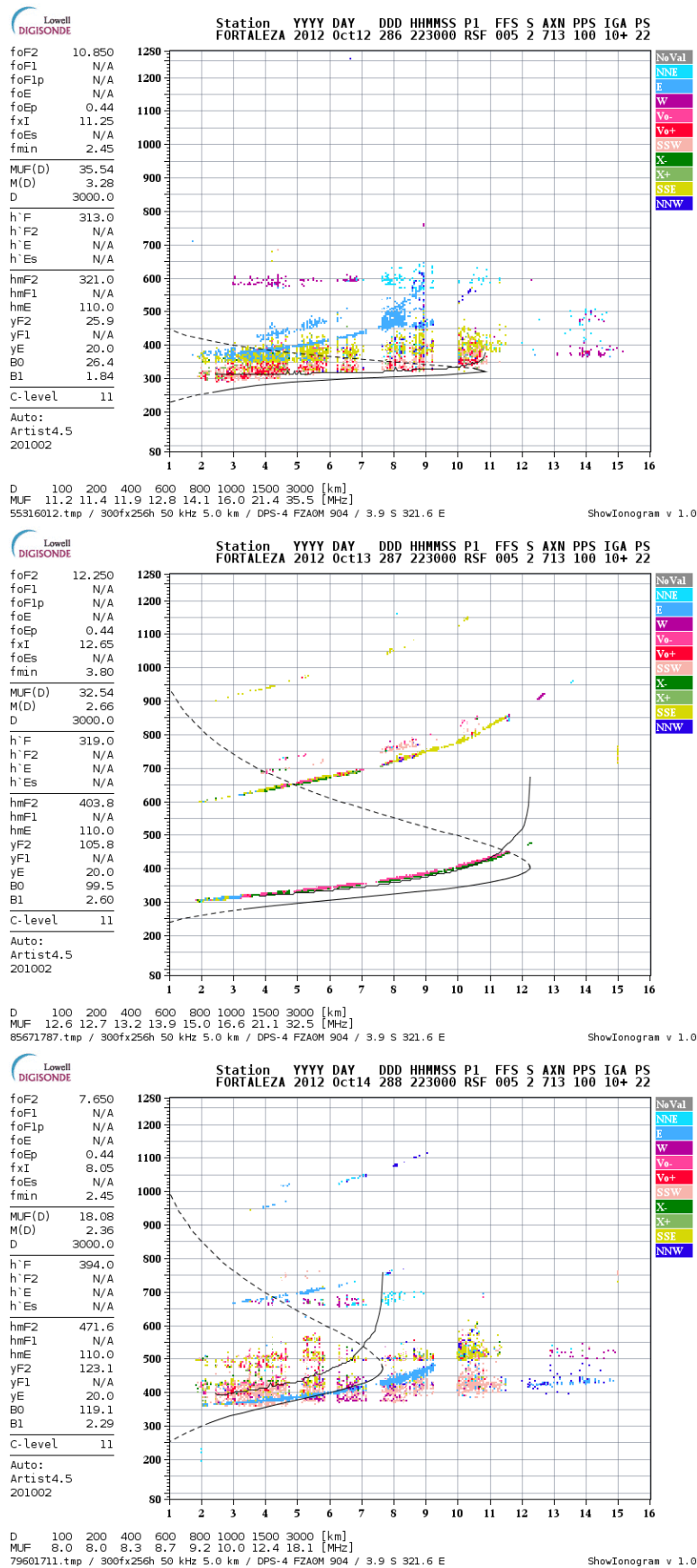


Figure 5. Ionograms of Fortaleza at 19:30LT (22:30UT) on 12 (the top panel), 13 (the middle panel), and 14 (the bottom panel) October 2012.

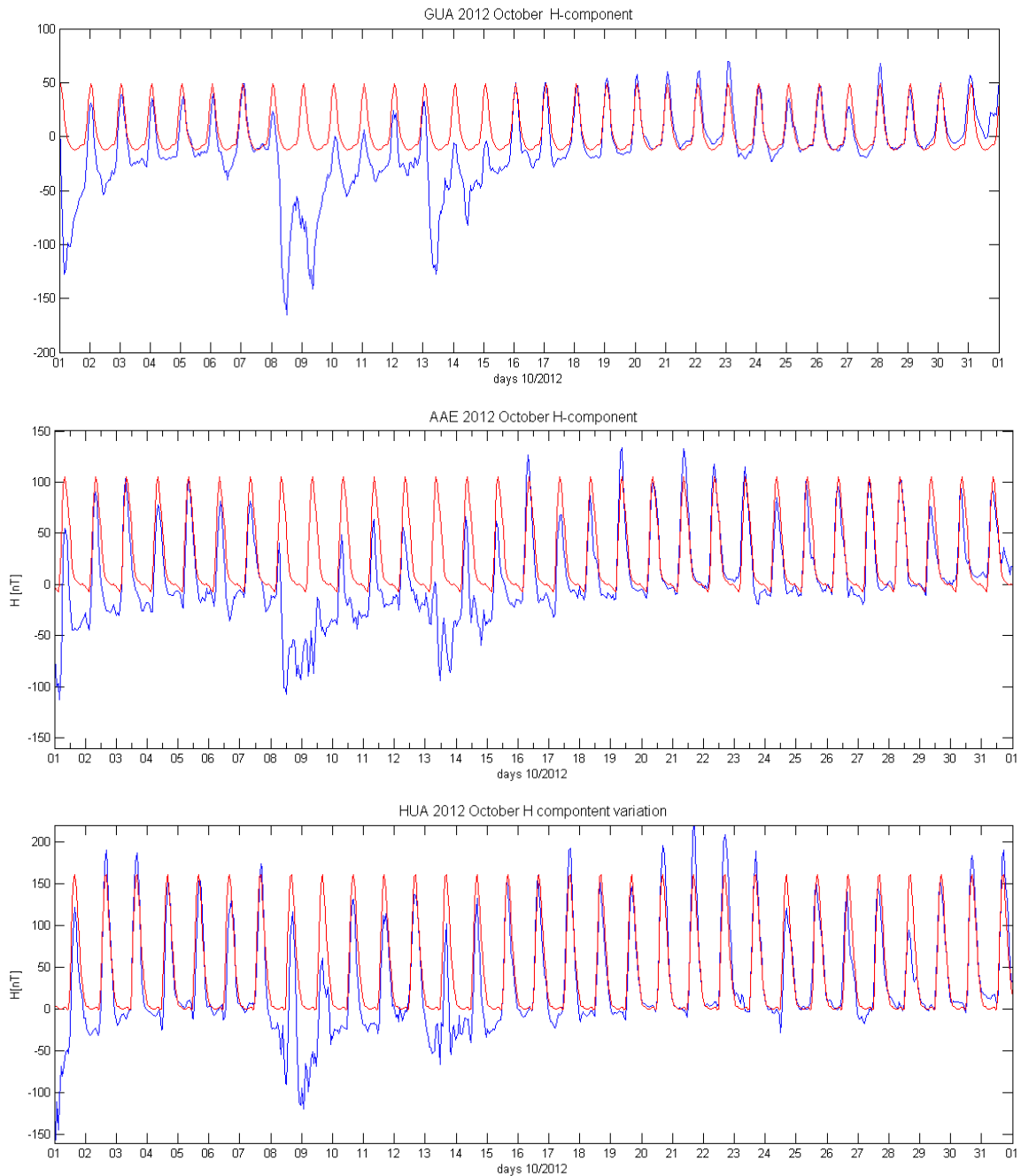


Figure 6. Variation of the geomagnetic field in October 2012, in low latitudes in the African sector (Addis Ababa), in the Asian sector (Guam), and in the America sector (Huancayo). The red line represents the regular variation of Sq and the blue line shows the observations.



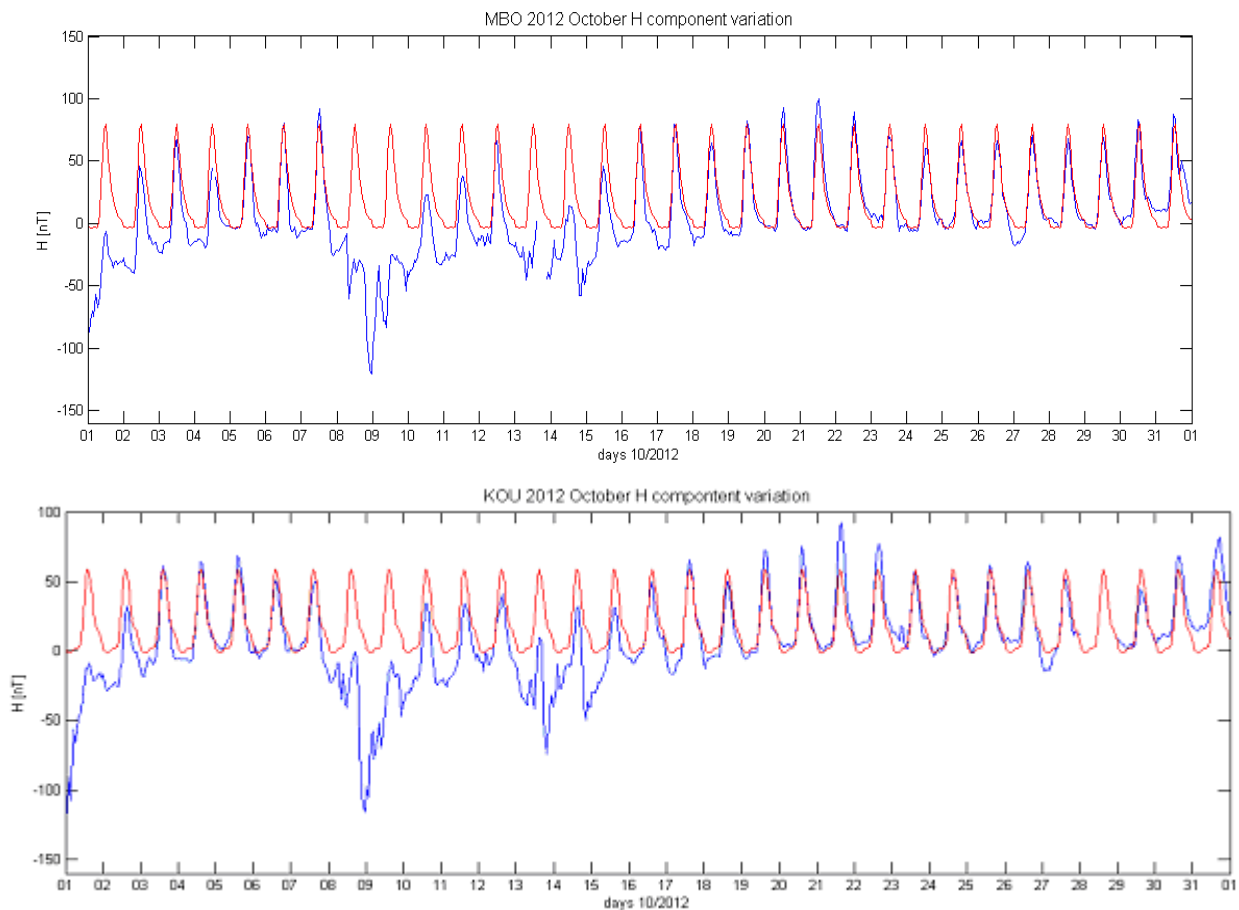


Figure 7. Variation of the Earth's magnetic field in October 2012, in latitudes of the Northern crest of ionization, in the African sector (M'Bour) and in the American sector (Kourou). The red line represents the regular variation of Sq and the blue line shows the observations.

The amplitude of the geomagnetic disturbance on 13 October associated with the second HSSWS was smaller at HUA ( $|H| \sim 60$  nT) than that at MBO ( $|H| \sim 70$  nT, considering the last value before the gap) and at KOU ( $|H| \sim 80$  nT). The amplitude of the geomagnetic disturbance  $|H|$  at AAE was  $\sim 100$  nT and at GUA was  $\sim 120$  nT, respectively. They were only 33% greater than the amplitude at MBO and at KOU. On 14 October,  $|H|$  ( $\sim 80$  nT) at GUA was still larger than  $|H|$  ( $\sim 50$  nT) at MBO, at AAE, and at KOU.

Figure 8 is composed by two panels, the  $D_{\text{iono}}$  (blue curve) is superimposed to the disturbance  $D_{\text{dyn}}$  (red curve) for the period between 11 and 15 October (see equations 6 and 7). October 11 and 15 were two magnetic quiet days, with an Am index equal to 10 and 12, respectively. The day-to-day variation can be estimated by the fluctuations observed during the magnetic quiet days with the Am index between 20 nT and -20 nT. The variations of both  $D_{\text{iono}}$  and  $D_{\text{dyn}}$  were similar for those two days. The fluctuations of the equivalent current system  $DP_2$  (Nishida, 1968) were observed on  $D_{\text{iono}}$ .

In the early morning on 13 October, the  $D_{\text{iono}}$  at MBO and at KOU presented a large variation ( $\sim 60$  nT) around 06:00UT and a negative variation in the afternoon. This is the signature of a westward ionospheric electric current. The disturbance in the

afternoon ( $\sim -60$  nT) was greater than the day-to-day variation. This observation can be interpreted as the effect of the Disturbance Dynamo Electric Field (DDEF) of the ionosphere (Blanc and Richmond, 1980). Blanc and Richmond's model predicts a disturbed westward ionospheric electric current during the daytime in low latitudes.

Figure 9 shows the superposition of Diono at MBO and at KOU. In the early morning from 00:00UT to 06:00UT on 13 October, Diono at MBO and at KOU was similar and grew up at the same time. This is the characteristic of the Prompt Penetration Electric Field (PPEF) which varies in universal time (Nishida et al., 1966; Nishida, 1968; Vasyliunas, 1970). Around 11:00UT (10:00LT at MBO and 08:00LT at KOU), variations of Diono at MBO and at KOU were separated in time, but exhibited a similar pattern. The variation at KOU was similar to that at MBO with a delay for several hours. This fact confirms our interpretation of the afternoon disturbance as the effect of the DDEF (Blanc and Richmond, 1980). The ionospheric disturbance dynamo varies in local time. In the morning on 13 October, the positive disturbance of Diono was associated with a large decrease of the SYM-H index. SYM-H index decreased from -30 nT at 00:00UT to -120 nT around 08:00UT and then increased. The PPEF was related to this storm.

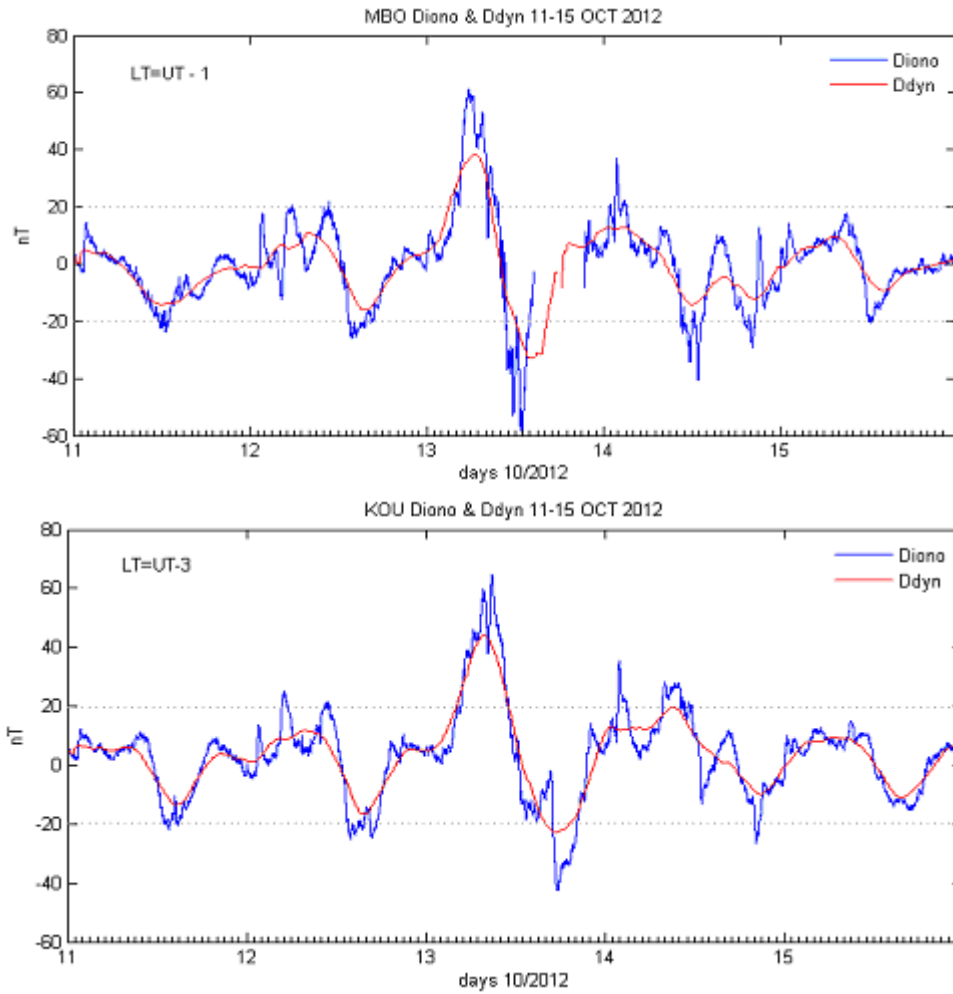


Figure 8.  $D_{iono}$  (blue curve) and  $D_{dyn}$  (red curve) for the period between 11 and 15 October 2012 at MBO (the top panel) and at KOU (the bottom panel).

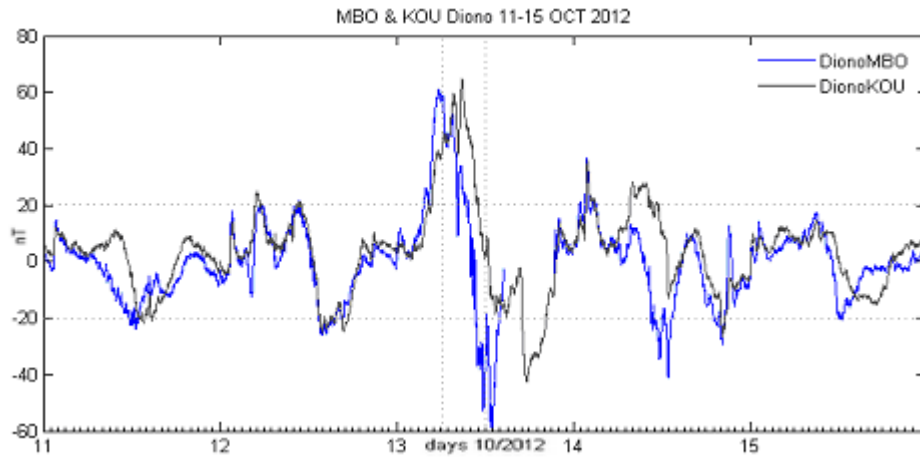


Figure 9.  $D_{iono}$  at MBO (blue curve) and  $D_{iono}$  at KOU (black curve) are superimposed for the period between 11 and 15 October 2012.

#### 4. Discussion

In this paper, we studied the 13 October 2012 case with the global geophysical context (Figure 2). This event was preceded by the arrival of a CME in the early morning and by the arrival of a HSSWS in the evening on 9 October. This case presents similar features of the previously analyzed case on 14 October 2013 associated with the arrival of a HSSWS to the Earth during daytime (Azzouzi et al., 2015).

We analyzed the variation of the  $h^{\prime}F$  and showed the presence of spread F, in low latitudes and in equatorial latitudes, using the ionosonde data in the African, Asian, and American sectors (Figures 3a, 3b, 4, and 5). The impact of the HSSWS was observed on 13 October 2012 in the African sector (Ascension Island) and in the Eastern American sector (Fortaleza). In this case and the 14 October 2013 case (Azzouzi et al., 2015), the HSSWS effect was to stop the lift of the F layer in the post sunset. The absence of spread F at the time of the PRE was observed on Figures 4 and 5. During a geomagnetic disturbance, there are large electric fields transmitted from the auroral zone to the equator (Fejer et al., 1983). A westward electric field from auroral origin inhibits the eastward regular field and stops the ascent of the F layer. There is no generation of irregularities as a consequence. Abdu et al. (2009) observed, in equatorial latitudes, during a large increase of auroral currents, a strong downward vertical drift of the F layer associated to the disappearance of spread F (as shown in Figure 1 of their paper). This downward vertical drift is interpreted as the effect of the prompt penetration of a westward electric field, as explained in the introduction of Azzouzi et al. (2016). On the 13 October 2012 case, disappearance of irregularities was detected in the ROTI (Figure 8 of Azzouzi et al. (2016)). Previously, Azzouzi et al. (2015) studied the period in October 2013 and found that there was ionospheric scintillation over all Africa in the analyzed period except on 14 October. No uplift of the F layer after sunset on 14 October 2013, like on 13 October 2012 was observed at Ascension Island. Adohi et al. (2008) and Tanoh et al. (2015) found similar events with no uplift of the F layer at Korhogo. They found such events occurred only eight times in 365 days (occurrence rate, 2.2%) in 1995, during the descending phase of the solar cycle 22.

Two main physical processes, connecting auroral and equatorial latitudes, produce disturbed electric fields: 1) the prompt penetration of magnetospheric convection, the PPEF (Nishida, 1968; Vasyliunas, 1970) and 2) the DDEF (Blanc and Richmond, 1980). Concerning the mechanism of the PPEF, the direction of the electric field transmitted to the low latitudes, depends on universal time of the event. The geomagnetic disturbance related to the PPEF is observed at the same time in all longitude sectors (see Azzouzi et al., 2015). Before the shielding becomes effective (phase of undershielding of the PPEF), the transmitted electric field has the polarity of the dawn-dusk convection electric field (eastward during the

day until 21:00LT and westward in the night sector). The over-shielding electric field (Kelley et al., 1979; Kobera et al., 2000) is related to the decline of the convection electric field. The transmitted electric field of the PPEF is westward in the day side and is eastward in the night side. Finally, the transmitted electric field related to the DDEF (Blanc and Richmond, 1980; Sastri, 1988) is westward during the daytime, turns eastward around 22:30LT, and remains eastward until the end of the night (Huang et al., 2005). Abdu et al. (2009) observed the suppression of the pre-reversal drift and the suppression of the spread F by an effect of the PPEF. In our case like in the case studied by Azzouzi et al. (2015), the suppression of spread F is related to the DDEF associated to a HSSWS.

To study the geomagnetic variations, we used the magnetometers at MBO (LT=0UT-1) and at KOU in French Guyana (LT=0UT-3). They are in the same longitude sector than Ascension Island and Fortaleza in Brazil, respectively. In Figure 8,  $D_{\text{dyn}}$  (red curve) and  $D_{\text{iono}}$  (blue curve) variations observed at MBO and at KOU are superimposed for the period between 11 and 15 October 2012. On 13 October 2012, a comparable significant disturbance was observed at MBO ( $H \sim -60$  nT) and at KOU ( $H \sim -50$  nT) (see Figure 8). The disturbance of the equivalent ionospheric electric current,  $D_{\text{iono}}$  was positive during the morning hours ( $\sim 6:00$ UT) and negative in the afternoon. This positive disturbance occurred during the main phase of the geomagnetic storm which started around 00:00UT on 13 October at MBO and at KOU and varied simultaneously (Figure 9). This is evidence that the disturbance of  $D_{\text{iono}}$  was due to the PPEF. Abdu et al. (2013) studied the development of sporadic E layer in the early morning, during storms, associated to a westward PPEF. Foster and Rich (1998) found, at the beginning of a storm, the effect of an eastward PPEF at middle latitudes and Huang (2009), like Foster and Rich (1998) found a similar effect of an eastward PPEF, in low latitudes, at the beginning of substorms. The direction of the transmitted PPEF depends on the phase of the disturbance.

The negative excursion of  $D_{\text{iono}}$  in the afternoon on 13 October, which is dependent on local time (Figure 9), can be interpreted by the DDEF (Blanc and Richmond, 1980). This disturbance is westward during the daytime and turns eastward around  $\sim 22:30$ LT (Huang et al., 2005). Such a disturbance was previously observed, in April 2010, for several days by Fathy et al. (2014). Indeed, the DDEF lasts and influences the ionosphere for one or two days after a storm (Scherliess and Fejer, 1997). Fejer et al. (2008a, 2008b) have determined the equatorial vertical plasma drift during geomagnetic quiet periods and geomagnetic disturbed periods, with the data from the ROCSAT satellite. They built a model of the DDEF. They found the same result by Richmond and Blanc (1980) and Huang et al. (2005). The plasma moves upward during nighttime ( $\sim 22:00$ UT to 6:00UT) and moves downward during daytime ( $\sim 6:00$ UT to 22:00UT). Around 19:00LT, Fejer et al. (2008b) found a maximum of the downward

vertical drift, i.e. a maximum of a westward electric field which is opposite to the regular eastward electric field. This westward electric field causes the inhibition of ionospheric scintillations. An upward/downward vertical drift corresponds to an eastward/westward electric field and to a positive/negative variation of the H component of the geomagnetic field.

## 5. Summary and conclusion

In this paper we studied in detail the behavior of the ionospheric F layer and of the geomagnetic field at equatorial observatories under the influence of a HSSWS on 13 October 2012.

We found the following results:

- The HSSWS affected the rising of the F layer at the observatories of Ascension Island (Africa) and Fortaleza (Eastern America). It stopped the lift of the F layer at Ascension Island, and delayed the ascent of the F layer for approximately two hours at Fortaleza. It caused the disappearance of the spread F during the whole night at Ascension Island and the disappearance of the spread F during the beginning of the night at Fortaleza, when the ascent of the layer was delayed.
- The HSSWS affected the geomagnetic field and produced an anti Sq circulation at MBO (the African sector) and at KOU (the Eastern American sector).
- No effect of the HSSWS was observed at Guam (the Asian sector) and at Jicamarca (the Western American sector).
- These observations highlight the fact that the impact of the HSSWS was regional and affected the observatories with local time between LT=OUT+3 and OUT-3. They corresponds to a longitude sector between 315°E and 45°E.
- The time delay of the geomagnetic disturbance in the afternoon between MBO and KOU shows that this disturbance varied in local time. This is the particularity of the DDEF of the ionosphere (Blanc and Richmond, 1980).
- In the early morning on 13 October 2012, a disturbance of the geomagnetic field was observed at MBO and KOU at the same time. This is the signature of the PPEF which varies in universal time.
- This work shows the interest of using geomagnetic data to determine physical processes in the ionosphere in the dayside. The geomagnetic signature of the PPEF is different from the magnetic signature of the DDEF.
- The ionosonde and magnetic observations were in good agreement with the GPS observations (see Azzouzi et al., 2016) and these data added precisions on the physical mechanisms activated by the HSSWS.

While Azzouzi et al. (2015) analyzed the impact of a HSSWS only in the African sector, in the present study, we studied the equatorial ionosphere response at the planetary scale and the longitudinal impact of a

HSSWS in the equator using the longitudinal chains of equatorial magnetometers and ionosondes.

The next step of this work is to develop statistical studies and modeling of this kind of disturbances with a global model such as the Thermospheric Ionospheric Electrodynamic Global Circulation Model (TIEGCM).

## Acknowledgment

Results from geomagnetic data presented in this paper rely on the data collected at AAE, GUA, KOU, HUA and MBO magnetic observatories. We thank Addis Abeba University, Institut de Physique du Globe de Paris, U.S. Geological Survey, Instituto Geofísico del Perú, Centre National d'Etudes Spatiales, and Institut de Recherche pour le Développement for supporting their operations and the INTERMAGNET for promoting high standards of magnetic observatory practice ([www.intermagnet.org](http://www.intermagnet.org)).

The authors thank the Helmholtz-Zentrum Potsdam of Deutsches GeoForschungsZentrum for Adolf-Schmidt-Observatorium for the International quiet days, the International Service for Geomagnetic Indices, the World Data Center for Geomagnetism, Kyoto and the Ecole et Observatoire des Sciences de la Terre (Strasbourg) for providing the geomagnetic indices used in this study.

The authors thank the LGDC and all the providers of the ionosonde data.

Our sincere thanks go to all members of the LPP/Polytechnique/ UPMC/CNRS, Telecom Bretagne-Brest University, the Ecole Mohammadia d'Ingénieurs (EMI)/Université Mohammed V Agdal Rabat-University, and the Abdus Salam International Centre for Theoretical Physics (ICTP), for their ceaseless support. This work was supported by a part of the JSPS Core-to-Core Program (B. Asia-Africa Science Platforms), Formation of Preliminary Center for Capacity Building for Space Weather Research.

This is IPGP contribution n.3718.

## References

- Abdu, M. A., de Medeiros, R. T., Sobral, J. H. A., Bittencourt, J. A.: 1983, *J. Geophys. Res.*, **88**, A11, 9197.
- Abdu, M. A., Kherani, E. A., Batista I. S., and Sobral, J. H. A.: 2009, *Geophys. Res. Lett.*, **36**, L19103, doi:10.1029/2009GL039919.
- Abdu, M. A., Souza, J. R., Batista, I. S., Fejer, B. G., and Sobral, J. H. A.: 2013, *J. Geophys. Res.*, **118**, 2639, doi:10.1002/jgra.50271.
- Adohi, J.-P., Vila, P. M., Amory-Mazaudier, C., and Petitdidier, M.: 2008, *Ann. Geophys.*, **26**, 1777.
- Azzouzi, I., Migoya-Orué, Y., Amory Mazaudier, C., Fleury, R., Radicella, S., Touzani, A.: 2015, *Adv. Space Res.*, **56**, 2040, doi:10.1016/j.asr.2015.06.010.
- Azzouzi, I., Migoya-Orué, Y., Coisson, P., Amory Mazaudier, C., Fleury, R., Radicella, S.: 2016, submitted to *Sun and Geosphere*.
- Blanc, M., and Richmond, A. D.: 1980, *J. Geophys. Res.*, **85**, A4, 1669.
- Davis, C. J., Davies, J. A., Owens, M. J., and Lockwood, M.: 2012, *Space Weather*, **10**, S02003, doi:10.1029/2011SW000737.
- Doherty, P. H., Delay, S. H., Valladares, C. E., and Klobuchar, J. A.: 2000, Ionospheric scintillation effects in the equatorial and auroral regions, 13th International Technical Meeting of

- the Satellite Division of The Institute of Navigation (ION GPS 2000), p. 662.
- Fejer, B. G., Jensen, J. W., and Su, S. Y.: 2008a, *J. Geophys. Res.*, 113, A05304, doi:10.1029/2007JA012801.
- Fejer, B. G., Jensen, J. W., and Su, S.-Y.: 2008b, *Geophys. Res. Lett.*, 35, L20106, doi: 10.1029/2008GL035584.
- Fathy, I., Amory-Mazaudier, C., Fathy, A., Mahrous, A. M., Yumoto, K., and Ghamry, E.: 2014, *J. Geophys. Res.*, 119, doi:10.1002/2013JA019510.
- Foster J. C., and Rich, F. J.: 1998, *J. Geophys. Res.*, 103, A11, 26367.
- Grandin, M., Aikio, A. T., Kozlovsky, A., Ulich, T., and Raita, T.: 2015, *J. Geophys. Res.*, 120(12), 10669, doi: 10.1002/2015JA021785
- Huang, C. M., Richmond, A. D., and Chen, M. Q.: 2005, *J. Geophys. Res.*, 110, A05312, doi:10.1029/2004JA010994.
- Huang, C. S.: 2009, *Geophys. Res. Lett.*, 36, L18102, doi:10.1029GL040287.
- Kelley, M. C., Fejer, M. C., and Gonzales, C. A.: 1979, *J. Geophys. Res.*, 6(4), 301.
- Kelley, M. C., Ilma, R. R., and Crowley, G.: 2009, *Ann. Geophys.*, 27, 2053.
- Kobeia, A. T., Richmond, A. D., Emery, B. A., Peymirat, C., Luhr, H., Moretto, T., Hairston, M., Amory-Mazaudier, C.: 2000, *J. Geophys. Res.*, 105, A10, 22979.
- Lanzerotti, L.: 2007, *Space Weather*, 5, S06005, doi: 10.1029/2007SW000342.
- Le Huy, M., and Amory-Mazaudier, C.: 2005, *J. Geophys. Res.*, 110, A10301.
- Liu, J., Chen, R., Wang, Z., and Zhang, H.: 2011, *GPS Solutions*, 15(2), 109.
- Mayaud, P.N.: 1980, *Derivation, Meaning and Use of Geomagnetic Indices*, Geophysical Monograph series, Vol 22, AGU, Washington DC.
- Menvielle, M., Iyemori, T., Marchaudon, A., Nose, M.: 2011, in M. Manda and M. Korte (Eds.), *Geomagnetic indices, in Geomagnetic Observations and Models*, Special Sopron Book Series 5, Springer, Dordrecht Heidelberg London New York, doi: 10.1007/978-90-481-9858-0\_8.
- Migoya-Orué, Y. O., Radicella, S. M., and Coisson, P.: 2009, *Ann. Geophys.*, 27, 3133.
- Nishida, A., Iwasaki, N., and Nagata, N. T.: 1966, *Ann. Geophys.*, 22, 478.
- Nishida, A.: 1968, *J. Geophys. Res.*, 73, 1795.
- Sastri, J. H.: 1988, *Ann. Geophys.*, 6, 635.
- Scherliess, L., and Fejer, B. G.: 1997, *J. Geophys. Res.*, 102(A11), 24037.
- Tanoh, K. S., Adohi, B. J-P., Coulibaly, I. S., Amory-Mazaudier, C., Kobeia, A. T., and Assamoi, P.: 2012, *Ann. Geophys.*, 33, 143.
- Vasyliunas, V. M.: 1970, in M. McCormac (Ed.), *Mathematical models of magnetospheric convection and its coupling to the ionosphere*, in *Particles and Fields in the Magnetosphere*, Springer, New York, p. 60.
- Vestine, E.: 1947, *The Geomagnetic Field, Its Description and Analysis*, Carnegie Institute, Washington, DC, USA.